Journal Pre-proofs

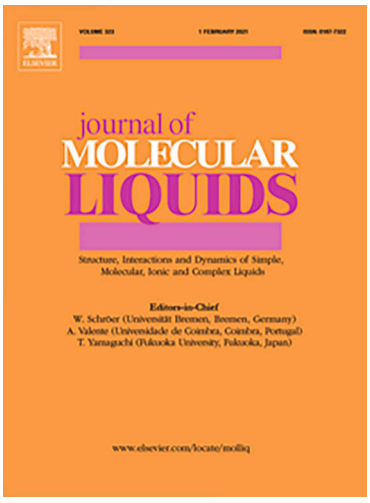

Colloidal dendritic nanostructures of gold and silver for SERS analysis of water pollutants

Tiago Fernandes, Sara Fateixa, Marta Ferro, Helena I.S. Nogueira, Ana L. Daniel-da-Silva, Tito Trindade

PII: S0167-7322(21)01332-5
DOI: https://doi.org/10.1016/j.molliq.2021.116608
Reference: MOLLIQ 116608

To appear in: *Journal of Molecular Liquids*

Received Date: 30 March 2021
Revised Date: 18 May 2021
Accepted Date: 26 May 2021

Please cite this article as: T. Fernandes, S. Fateixa, M. Ferro, H.I.S. Nogueira, A.L. Daniel-da-Silva, T. Trindade, Colloidal dendritic nanostructures of gold and silver for SERS analysis of water pollutants, *Journal of Molecular Liquids* (2021), doi: https://doi.org/10.1016/j.molliq.2021.116608

Colloidal dendritic nanostructures of gold and silver for SERS analysis of water pollutants

Tiago Fernandes[a], Sara Fateixa[a], Marta Ferro[b], Helena I. S. Nogueira[a], Ana L. Daniel-da-Silva[a], Tito Trindade[a]*

[a]Department of Chemistry, CICECO- Aveiro Institute of Materials, University of Aveiro, 3810-193 Aveiro, Portugal
[b]Department of Materials and Ceramics Engineering, CICECO-Aveiro Institute of Materials, University of Aveiro, 3810-193 Aveiro, Portugal

Graphical Abstract

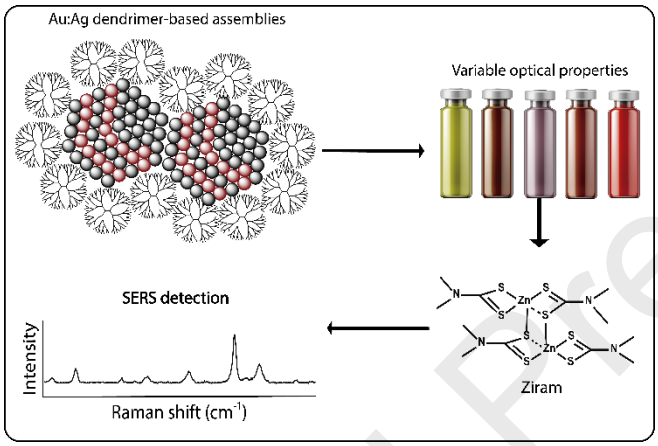

Abstract

Surface Enhanced Raman Scattering (SERS) using colloidal metal (Ag, Au) nanoparticles has been regarded as a powerful method for detecting organic pollutants at vestigial levels. Although less investigated, the controlled synthesis of binary nanostructures comprising two metals provides an alternative route to SERS platforms with tuned surface plasmon resonances. Here, we demonstrate that the use of dendrimers allows the formation of distinct combinations of Ag:Au nanostructures that are composed of smaller metal nanocrystals. Our research highlights the role of the dendrimer macromolecules as a multipurpose ligand in the generation of such hybrid nanostructure, including as a reducing agent, an effective long-term colloidal stabilizer and as a molecular glue for interconnecting the primary metal nanocrystals. Noteworthy, the dendrimer-based Ag:Au hybrid nanostructures are more SERS sensitive as compared to the corresponding colloidal blends or to the single-phase metals, as

revealed by using molecular pesticides as analytes in spiked water samples. We suggest that the high SERS sensitivity of the hybrid nanostructures is due to interparticle plasmonic coupling occurring between the primary metal nanoparticle aggregates, whose arrangement is templated by the presence of the dendrimer macromolecules.

Keywords: Metal Colloids; Dendrimers; Raman spectroscopy; SERS; Pesticides.

1. Introduction

Colloidal metal nanoparticles display unique optical properties that allows the manipulation of light-matter interactions for multiple applications across several fields[1–6]. In recent years, innovative strategies have been proposed where such plasmonic nanoparticles were used as building blocks of nanoassemblies that exhibit optical properties due to their collective behaviour[7–9]. This type of nanoassemblies exhibit a near-field coupling behaviour due to the packing of individual metal particles, resulting in an intensification of the electromagnetic field in nanoparticle junctions, also called hot spots. Because Raman scattering is a relatively weak inelastic phenomenon, such type of optical behaviour is of particular interest in SERS either for spectroscopic characterization or to probe target molecules that became adsorbed (or nearly located) in such metal nanojunctions[10–12]. Indeed, the Raman band enhancement observed for nanoparticle assemblies used as substrates might be of such magnitude that allows single-molecule detection[13–15]. This led to intensive research in developing plasmonic nanoassemblies capable of sensing a variety of molecules including dyes[16–19], pesticides[20–22] or biological molecules, such as nucleic acids or proteins[23–26]. The vast majority of these assemblies are formed using metal nanoparticles of a single metal (typically Au or Ag) but considerably less work has been devoted to colloidal nanoalloy assemblies as SERS probes[27–33].

Several works have explored the SERS performance of alloyed materials when compared with their monometallic counterparts[34–36]. For example, Gao et al. explored the SERS performance of Au-Ag alloy nanospheres for the detection of benzidine in artificial wastewater and compared it with core-shell and monometallic counterparts[34]. The authors have found that the Raman signals' intensity decreased

with time for the Ag and the core-shell nanoparticles due to oxidative etching, while the Au nanoparticles displayed limited SERS performance due to small extinction cross sections. On the other hand, the alloyed nanoparticles displayed superior SERS activity with high stability along time despite the oxidative conditions present[34]. Hence, the formation of Au:Ag nanoalloys seems an effective strategy to explore SERS as an analytical tool, which may be complementary to the use of single-metal phase probes. However, the controlled assembly of the individual nanoparticles into colloidal stable entities might be challenging to achieve using conventional methods, resulting in poor reproducibility of the SERS studies [37]. In order to obtain assemblies of long-term colloidal stability while retaining their plasmonic properties, polymers of various classes have been employed as stabilizing agents[38–40]. The poly(amidoamine) (PAMAM) dendrimers belong to a highly branched synthetic macromolecules class, which are monodispersed in terms of molecular weight and whose size, inner cavity and surface chemistry can be adjusted during the synthesis. Consequently, PAMAM dendrimers have been regarded as useful molecular templates and stabilizers to prepare colloidal metal nanoparticles[41]. In addition, the tuneable surface chemistry of dendrimers can be explored to promote chemical functionalization or to entrap molecules of interest.

Over the last few years, metal colloids have been explored in the SERS detection of water pollutants, such as molecular pesticides dissolved in aqueous systems[42–45]. For example, pesticide formulations based on dithiocarbamate compounds belong to a subclass of carbamate pesticides that are extensively used as fungicides or insecticides in agriculture. Namely, the pesticides thiram and ziram belong to this class of pesticides where thiram is a thiuram disulphide and ziram is a zinc(II) complex of dimethyldithiorcarbamic acid. The screening of this class of pesticides in water samples is usually accomplished by time-consuming large-scale analytical equipment such as high-performance liquid chromatography (HPLC) and mass spectrometry (MS)[46]. These methods are either expensive or require skilled personnel, restricting their fast implementation or *in situ* analysis. SERS has proved to be an alternative analytical technique for the trace detection of analytes in aqueous samples, given its easy implementation and high sensitivity. In previous work, we have demonstrated the potential of dendrimer-based gold systems for the SERS detection of chemical pesticides under variable operational conditions[47]. Herein, binary Ag:Au dendrimer-based

assemblies have been investigated for the SERS detection of ziram and thiram in water samples. Not only the design of such binary nanostructures makes this system morphologically distinct from the monometallic counterparts, but they also show a better SERS sensitivity.

2. Experimental section

Materials

The following chemicals were used without further treatment: G5-NH_2 PAMAM dendrimers (Dendritech, Midland, MI, USA); Tetrachloroauric(III) acid trihydrate ($HAuCl_4 \cdot 3H_2O$, 99.9%, Sigma-Aldrich); Silver nitrate ($AgNO_3$, Sigma-Aldrich, >99.0%) Ziram ($C_6H_{12}N_2S_4Zn$, Sigma-Aldrich, ≥99.5%); Thiram ($C_6H_{12}N_2S_4$, Sigma-Aldrich, ≥98.0%). Colloids of gold, silver and their alloys were prepared using ultrapure water (18.2 MΩ·cm, 25 °C, MilliQ, Millipore). Safety: pesticides are biocides that should be handled in small amounts and under adequate safety conditions due to their toxicity. Wastes of these compounds should be placed in containers for further treatment and disposable.

Synthesis of dendrimer-stabilized alloy nanoassemblies

The Au, Ag and alloy dendrimer-stabilized nanoassemblies were prepared according to previously reported procedures with several adaptations[47–49]. In this work, the particles were obtained using the 5th generation PAMAM dendrimer with primary amine terminal groups as a reducing and stabilizing agent. Typically, 60 mg of PAMAM dendrimer was added to 10 mL of ultrapure water and left to disperse under vigorous stirring (750 rpm) for 15 minutes. Then, various proportions of the Ag(I) and Au(III) salts were added to obtain either the monometallic or alloy nanoparticles by keeping as 20:1 the concentration ratio of metal to dendrimer (see Table 1). For example, for the particles with the 10:10:1 molar ratio (Ag:Au:PAMAM), 100 μL of aqueous $AgNO_3$ (227.3 mM) and 900 μL of aqueous $HAuCl_4 \cdot 3H_2O$ (25.4 mM) have been mixed. The reaction was then left to proceed for 24 hours at 25 °C. Throughout the reaction, it was observed a gradual change in colour for all the systems. When required, the reacting mixtures were extensively dialyzed for several days against deionized water up to a volume of 4 dm^3.

As control experiments, several blends of the monometallic nanoparticles were prepared by mixing Au and Ag dendrimer-stabilized nanoparticles with similar Au+Ag ratios to the alloy nanoassemblies.

Table 1 – The molar proportions used for the synthesis of the dendrimer-based assemblies. The blends of monometallic particles were prepared by mixing the Au/Ag nanoparticles based on similar proportions.

Sample ID (Au:Ag:PAMAM)	[Au] precursor (mM)	[Ag] precursor (mM)	[G5-NH_2 PAMAM] (mM)
0:20	0	4.77	0.21
5:15	1.14	3.41	
10:10	2.28	2.27	
15:5	3.55	1.14	
20:0	4.57	0	

Raman spectroscopy and microscopy studies

All the prepared dendrimer-based metal colloids were investigated as SERS substrates to detect thiram and ziram, which were used as model contaminants. The SERS experiments were carried out using the aqueous colloids as substrates. For thiram and ziram, stock methanol and acetone solutions were prepared respectively (1 mM), and then the following successive dilutions were done in ultra-pure water (thiram) or acetone (ziram) before adding to the colloids. No significant change in colloidal stability of the particles was observed after adding the pesticide samples. All SERS measurements were accomplished in a series of triplicates using freshly prepared dendrimer-based colloids and analyte solutions. The Raman spectra were acquired using 0.5 s and 1000 acquisitions, with the excitation wavelength set either at 532 nm or 633 nm and the laser power tuned to 35 mW and 25 mW, respectively. The SERS signal reproducibility and homogeneity of colloids deposited on a glass slide have been assessed by Raman imaging and using a thiram solution ($1x10^{-4}$ M). After solvent evaporation, the samples

were analysed under optimal conditions, whereas the particles with the molar ratios of 5:15 and 10:10 were probed using the 532 nm laser and the sample 15:5 by using the 633 nm laser. The Raman images were obtained by scanning the laser beam over an area of at least 15x15 μm using a laser power of 0.1 mW (at 532 nm) and of 0.3 mW (at 633 nm).

Instrumentation

The UV/VIS spectra were recorded using a GBC Cintra 303 UV/Visible spectrophotometer. The ^{1}H NMR spectra were acquired using a Bruker AVANCE III^{TM} HD - 500 MHz equipment by redispersing 15 mg of particles/dendrimer in D_2O. Transmission electron microscopy (TEM) and scanning electron microscopy (SEM) micrographs were obtained using the STEM HD2700 electron microscope operating at 200 kV. The High-resolution TEM micrographs and the selected area electron diffraction patterns (SAED), were acquired using the JEOL 2200FS HR-TEM. Energy dispersive X-ray spectroscopy (EDS) studies were performed using Bruker Esprit. Samples for electron microscopy and EDS were prepared by diluting the original colloids and depositing them on a carbon-coated Cu grid. Dynamic light scattering (DLS) and zeta potential measurements were accomplished using a Malvern Zetasizer Nano ZS equipped with a standard 633 nm laser. The X-ray powder diffraction (XRD) data were obtained using the PANalytical Empyrean X-ray diffractometer equipped with a Cu-Kα monochromatic radiation source at 45 kV/40 mA. Raman studies were accomplished using a combined Raman-AFM-SNOM confocal microscope WiTec alpha300 RAS+ with a Nd:YAG laser operating at 532 nm (35 mW) and a He:Ne laser operating at 633 nm (25 mW) as excitation sources. The inductively coupled plasma - optical emission spectroscopy (ICP-OES) analysis was carried out using the Jobin Yvon Activa M equipment.

3. Results and discussion

3.1 Colloidal synthesis and materials characterization

The preparation of binary Au:Ag nanostructures with distinct molar ratios was investigated to achieve metal colloids with variable optical responses. The use of the PAMAM dendrimer was explored to mediate different particle arrangements and thereby regulate near-field coupling effects. Here, two preparative routes have been employed in order to investigate Au:Ag dendrimer-stabilized hybrid colloids. First, the binary system was prepared by the co-reduction of both Ag(I) and Au(III) salts, using variable molar ratios in the same reacting mixture (termed as Au:Ag samples), in the presence of PAMAM without adding any additional reducing agent. Second, for comparative purposes, blends of Au and Ag colloids were prepared (termed as Au+Ag samples) and by using equivalent nominal amounts to those used in the co-reduction method. The PAMAM dendrimer was also used as a reducing and stabilizing agent in preparing the single metal colloids. PAMAM provides several amino terminal groups that form stable complexes with $AuCl_4^-$. This process limits the generation of free Cl^- through the formation of a strong ion pair between the Cl^- anion and the primary amines of PAMAM. Based on this process, it is possible to avoid the early precipitation of AgCl, even at conditions where the concentration of Cl^- is above the solubility product constant[48]. Moreover, the PAMAM dendrimer confers to the aqueous colloids a remarkable long-term colloidal stability.

It is instructive to compare the optical spectra of colloids prepared by both methodologies because we can draw some information concerning the type of metal nanostructures present in both cases. Figure 1 shows the UV/VIS spectra for the dendrimer-stabilized colloids as prepared by both strategies. The optical spectra of the blended colloids (Au+Ag samples) show LSPR bands peaked at 415 nm and 525 nm, respectively, for Ag and Au nanoparticles, whose relative intensity depends on the concentration of the respective monometallic colloids. Nevertheless, the UV/VIS spectra of the colloidal blends (Figure 1, right panel) mirror the summation of the spectra of the individual monometallic colloids. In particular, for the sample Au+Ag (5+15), the two LSPR bands of the nanometals are clearly distinguished and appear at about the same absorption maximum wavelength as the respective monometallic colloidal samples. This result is expected by considering that this sample resulted from the direct mixture of the Au and Ag colloids having PAMAM as an effective stabilizer, which avoids particle aggregation into intimate mixtures of the metal phases. On the other hand, the Au:Ag

samples, i.e. those obtained by co-reduction of the metal salts, show UV/VIS spectra (Figure 1, left panel) clearly distinct from those of the colloidal blends, which indicates that the hybrid samples are not segregated Au and Ag colloidal nanoparticles. The UV/VIS spectra of these nanostructures are characterized by band broadening across the 400-520 nm wavelength range. We interpret this result as a consequence of interparticle plasmon coupling in the metal colloids, which is negligible for the blended colloids due to the effective particle capping of the dendrimer in keeping distant the two types of metal nanoparticles. Although surface capping protection also occurs for the Au:Ag samples, in this case, the particles have been generated *in situ* in the presence of the dendrimer. Thus, the metal nanoparticles end up more intimately mixed at the nanoscale resulting in alloyed structures. Hence, the blended Au and Ag colloids result in metal nanoparticles well dispersed due to the presence of the dendrimer but, in the bimetallic Au:Ag systems, the particles are closer to each other because they have been prepared by co-reduction of the precursors. Therefore, the dendrimer can be regarded as a molecular “glue” for alloyed Au and Ag Nanoparticles that are close enough for plasmonic coupling, which also explains the absence of a well-defined absorption band ascribed to a specific alloy composition. The type of optical response reported for dendrimer-based Au/Ag nanostructures strongly depends on the experimental conditions used in their synthesis, which ultimately determine the type of metal nanostructure present in the colloid [50–53]. The distinction between the different types of binary metal nanostructures is not trivial and cannot be made solely based on optical measurements.[51,52]

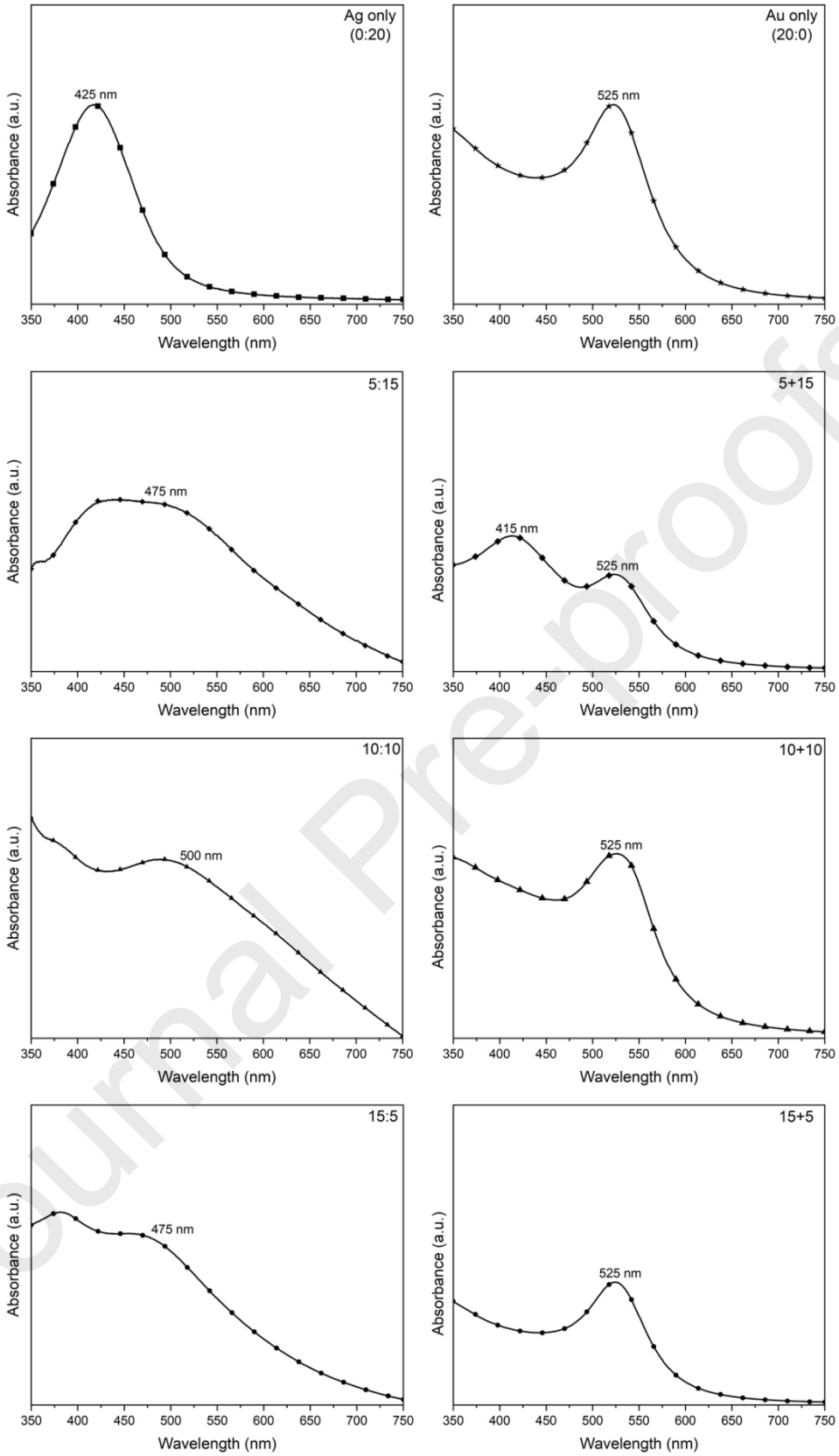

Figure 1 – UV-VIS spectra of metal colloids prepared in the presence of PAMAM dendrimer at the indicated relative nominal amounts of Au and Ag. The panel on the left corresponds to the binary Au:Ag nanostructures and the panel on the right corresponds to the colloidal blends.

The above discussion shows that the binary Au:Ag colloids are composed of nanostructures morphologically distinct from the monometallic colloids and their blends. As such, those nanostructures were investigated in more detail for their morphological characteristics, as shown in Figure 2 for a typical Au:Ag assembly using the 15:5:1 molar ratio of Au:Ag:PAMAM. The corresponding data for the binary Au:Ag systems with other molar ratios are shown in the Supporting Information (Figure S1-S4). Taking together the TEM and EDS data (Figure 2), the binary Au:Ag samples show as predominant morphologies, primary metal particles clustered into larger structures. Note the marked differences between the EDS maps of the Au:Ag nanostructures and those of the colloidal blends, as shown in Figure 2. While in the binary Au:Ag structures (Figure 2-B), the Au and Ag nanophases are randomly distributed over the assembly, the Au+Ag blends appear as segregated metal nanoparticles, showing smaller Au nanoparticles displaced from the bigger Ag particles. Hence, the above data indicate that this colloidal synthesis requires the co-reduction of the metal salts to promote the formation of hybrid Au:Ag nanostructures, with the dendrimer acting as molecular glue, as suggested by the previous discussion of the optical spectra. Hence, it is reasonable to assume that the clustering of the primary particles had occurred in solution, and it is not a consequence of sample preparation for microscopy. Indeed, the hydrodynamic diameter distribution, which is shown in Figure 2-E, confirms that such hybrid nanostructures are already present in the original colloid. In this case, the average hydrodynamic diameter of such nanostructures is about 131 nm, which is consistent with the electron microscopy results (Figure 2-A) that show hybrid aggregates (about 106 nm) composed of smaller primary metal particles (about 20 nm). The dendrimer-stabilized alloy nanoassemblies displayed good colloidal stability for extended periods of times while maintaining their optical properties (Supporting information, Figure S5). The presence of the dendrimer at the surfaces of the resulting assemblies was also confirmed by zeta potential analysis and SEM performed on the hybrid nanostructures (Supporting information, Figures S6 and S7), that clearly show clustered metal nanoparticles due to the presence of the dendrimer at their surfaces. Furthermore, the ^{1}H NMR of all samples exhibited the characteristic signals of the PAMAM dendrimer after purification through dialysis of the colloids (Figure 3). Interestingly, the ^{1}H NMR spectra of the hybrid nanoassemblies reveal slight differences

compared with the spectra of the monometallic counterparts. Firstly, the small shift of the C/c protons indicates the proximity to the dendrimer terminal groups to Au/Ag metal surfaces[54]. Also, the splitting of several signals may be attributed to a change in the coordination environment and close packing of several dendrimer assemblies observed during the formation of the hybrid structures[55].

Another interesting aspect suggested by the EDS maps concerns the distinct size range observed for the Au and Ag nanophases, either in the Au:Ag hybrid samples and colloidal blends. All the samples have shown more extensive regions corresponding to Ag nanophases than those corresponding to the Au nanophases, which are numerous but more dispersed. Moreover, an increase in the nominal Ag content also increases the Z-average (see SI material) of the final structures. On the other hand, the metal content in the bimetallic nanostructures as determined by ICP-OES (Table 1) revealed a Au:Ag molar ratio close to the nominal feeding ratios, but with the Au content consistently higher than the Ag content. This might be explained by taking into consideration the lower reduction potential ($Ag^+ \rightarrow Ag$) as compared to the potential ($AuCl^-_4 \rightarrow Au$), which also allows the occurrence of charge-transfer processes during the colloidal synthesis from the less noble metal (e.g. Ag) to the most noble one (e.g. Au).[56,57] Consequently, there is the extensive formation of Au, but a certain amount of unreacted Ag(I) remain in the reacting mixture, which is subsequently removed during the purification step. In the end, the binary Au:Ag nanostructures are characterized by a chemical composition dependent on the metal salts ratio employed in the synthesis. It should be recalled that metal alloying of Au and Ag is favoured due to the same face centred cubic lattices and similar lattice constants (Au: 4.08 Å; Ag: 4.09 Å). Consequently, in Figure 4, the XRD peaks observed at 38.1°, 44.2° and 64.5° corresponding to the (111), (200) and (220) planes are consistent with the presence of alloyed Au:Ag nanophases rather than a mixture of the pure metals; the corresponding data for the monometallic phases is also shown for comparison. In addition, the selected area electron diffraction (SAED) results presented in Figure 2-D shows a single face centred cubic pattern composed of dotted (larger particles), and diffuse (smaller particles) rings that matches well with the corresponding XRD diffraction pattern of the sample in consideration. All the characterization data presented above suggests that the bimetallic nanostructures prepared in this work are consistent with the presence of Au:Ag alloys.

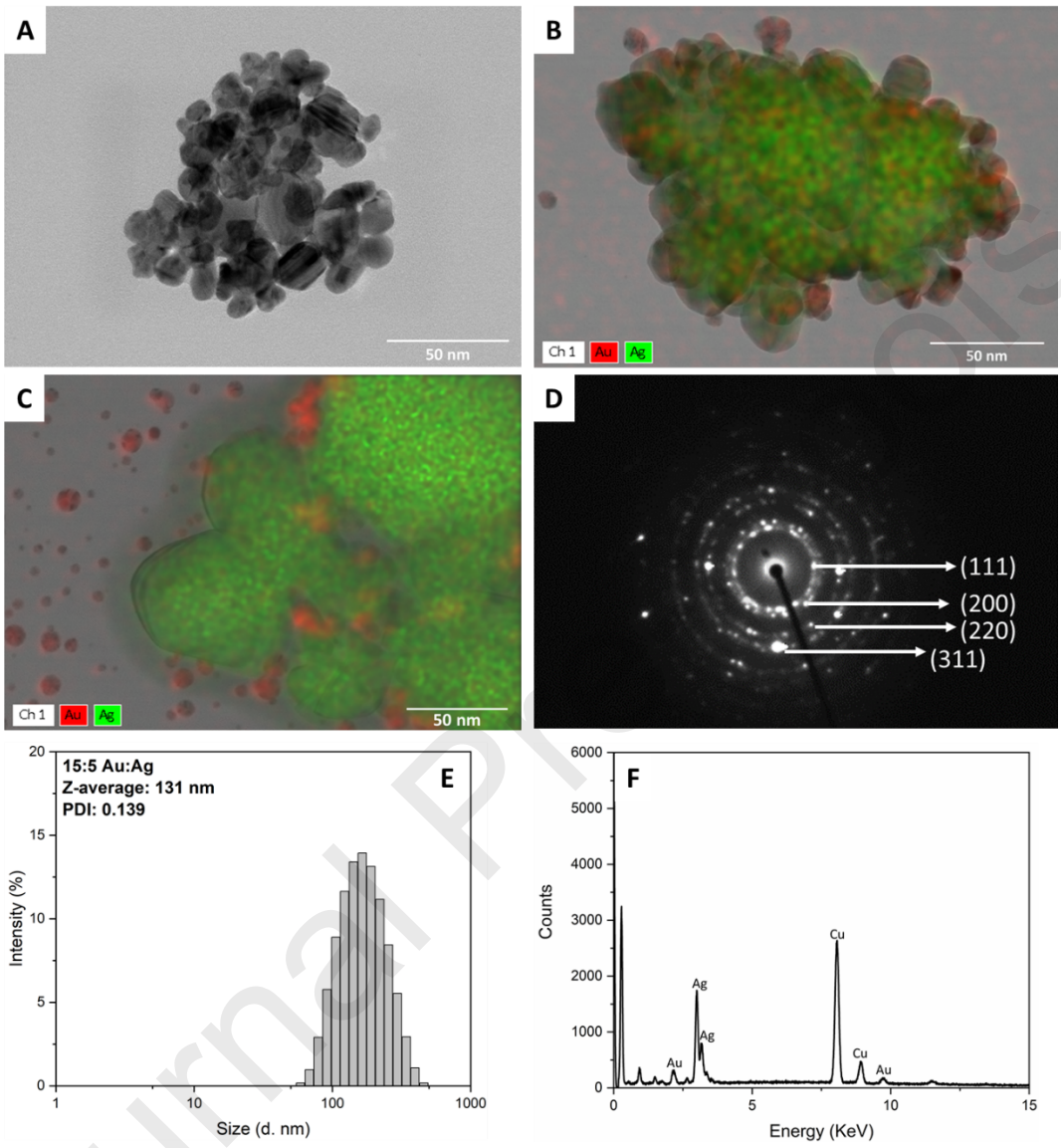

Figure 2- Typical electron microscopy images of the bimetallic dendrimer-stabilized nanoparticles of (A) 15:5:1 Au:Ag:PAMAM; EDS mapping of 15:5:1 Au:Ag:PAMAM nanoparticles (B) and of the Ag+Au blended colloids (10:10) (C). SAED pattern of corresponding 15:5:1 Au:Ag:PAMAM nanoparticles (D) along with its DLS data (E) and EDS spectrum (F).

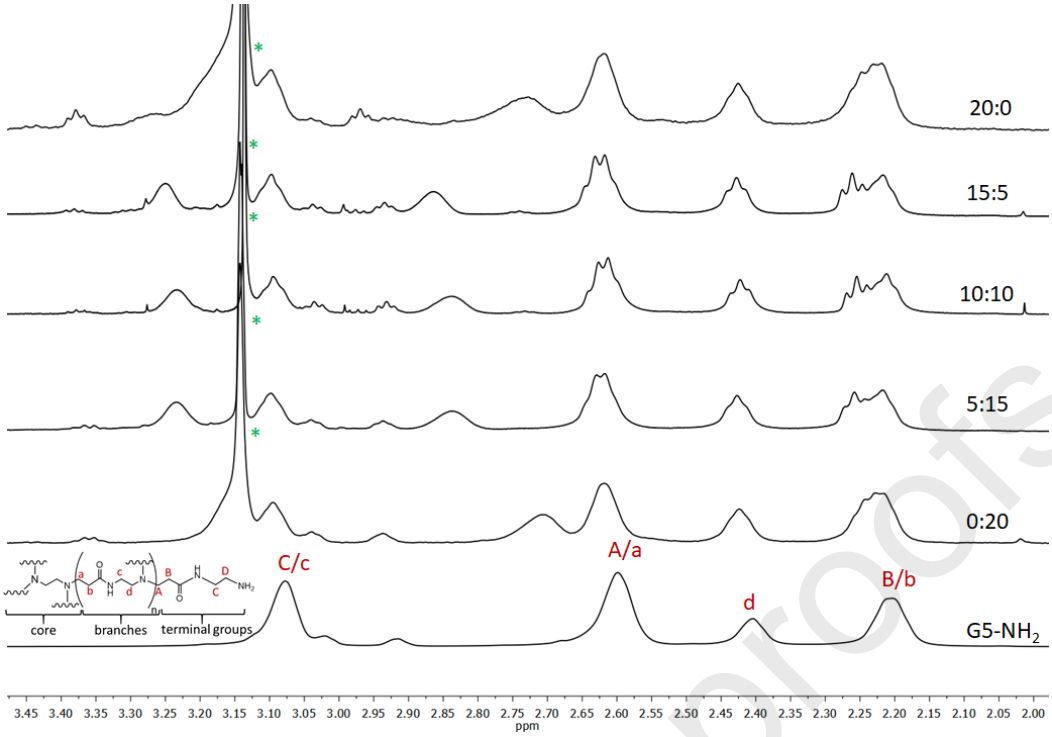

Figure 3 – ^{1}H NMR spectra of monometallic and bimetallic dendrimer-stabilized metal colloids (spectra identification using Au:Ag ratio; G5-NH_2 from a PAMAM dendrimer solution in D_2O).

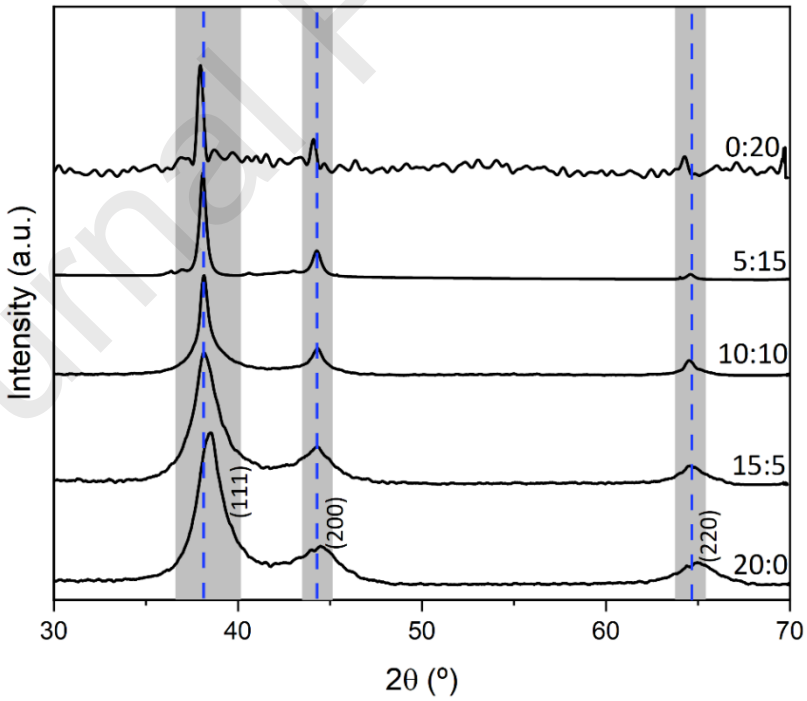

Figure 4 – Powder XRD patterns of monometallic and bimetallic dendrimer stabilized nanoparticles isolated from the respective colloids (sample identification using Au:Ag ratio).

Table 2 – Nominal and experimental Au:Ag molar ratios (ICP-OES) in the binary samples.

Au:Ag:PAMAM initial concentration proportion	Au:Ag nominal molar ratio	Au:Ag experimental molar ratio	
		Before dialysis	After dialysis
20:0:1	-	-	-
15:5:1	3.18	2.65 ± 0.05	5.32 ± 1.10
10:10:1	1.00	1.08 ± 0.18	2.07 ± 0.94
5:15:1	0.34	0.34 ± 0.01	1.26 ± 0.11
0:20:1	-	-	-

3.2 SERS studies using Au:Ag colloids as substrates

The Au:Ag hybrid nanoassemblies described above were investigated for the SERS detection of selected pesticides dissolved in water under irradiation in two distinct wavelengths (532 and 633 nm). For comparative purposes, the colloidal samples prepared by blending the Au and Ag colloids were also tested in similar conditions. All the SERS experiments were carried out using aqueous colloids containing a certain amount of the pesticide. First, the Raman spectra of the PAMAM stabilized metal colloids were recorded using both laser lines, showing that these colloids do not exhibit pronounced Raman signals in the spectral region of interest (Figure S8). Then, the SERS activity of the hybrid Au:Ag substrates was first tested to detect ziram, as detailed in Figure 5. The Raman bands in the SERS spectra of the dimethyldithiocarbamate anion from ziram were assigned according to the literature[58–61]: 343 cm^{-1} ν(Ag-S); 441 cm^{-1} δ(CSS); 565 cm^{-1} ν_{sym}(CSS); 935 cm^{-1} ν(CS); 1152 cm^{-1} ν(N-CH_3) + ρ(CH_3); 1386 cm^{-1} ν(CN) + δ_{sym}(CH_3); 1437 cm^{-1} δ_{asym}(CH_3) and 1515 cm^{-1} ν(CN). In Figure 5, we have used ziram powder as the reference, instead of an aqueous solution of this compound, due

to its low solubility in water at high concentration and to avoid Raman signal interference when using an adequate organic solvent. In comparison with the Raman spectrum of the powder, the SERS spectra show changes in the relative intensities of the bands, namely the Raman bands at 1386 cm^{-1} and 1515 cm^{-1} which are both enhanced in relation to the bands at 441 cm^{-1} and 568 cm^{-1}. The band at 1515 cm^{-1} is assigned to the ν(CN) mode arising from the thioureide form, which in solution is in tautomeric equilibrium with the dithiocarbamate anion [58,62]. It has been reported that the thioureide form is favoured upon complexation due to metal interaction trough the nitrogen electron lone pair [55]. The band's intensification at 1515 cm^{-1} suggests that the bidentate anion is the predominant adsorbate within the concentration range tested, using the Au:Ag colloids as substrates (Figure 5). This is in line with the shift for lower wavenumbers (≈20 cm^{-1}) of the band at 935 cm^{-1} in the SERS spectra of ziram, which is also indicative of the existence of bidentate complexes[55]. However, the monodentate form is also present as indicated by the less intense band at 1437 cm^{-1}, particularly noticeable under 532 nm excitation conditions and when using the Au:Ag:PAMAM colloids with molar ratio 5:15:1 (Figure 5-A). Note that Raman band enhancement was only observed for the Ag containing colloids and, in particular, in the bimetallic nanostructures. This is in line with the observation of the band 345 cm^{-1} assigned to the vibrational stretching of Ag-S.

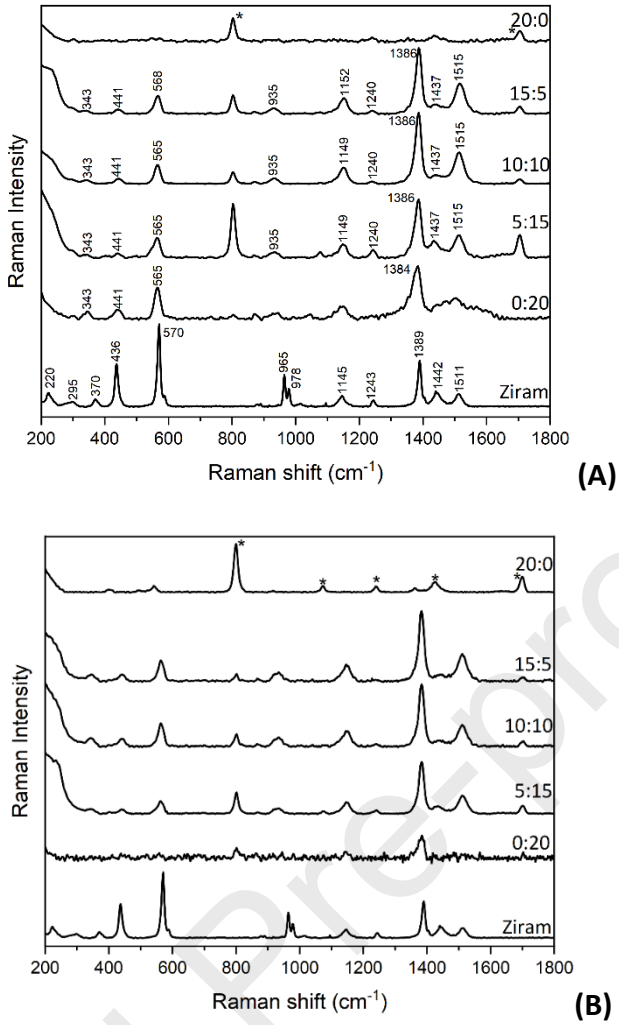

Figure 5 – SERS spectra of ziram (1x10^{-4} M) using Au:Ag binary nanostructures as substrates under 532 nm (A) and 633 nm (B) laser excitation. Conventional Raman spectrum of ziram powder is also shown at the bottom, in each pannel. The band marked with an asteric arises from residual solvent (acetone).

Figure 6 shows the Raman spectra of thiram using the Au:Ag colloids as the substrates and also for a thiram solution. The most prominent vibrational bands in the SERS spectra were assigned accordingly to literature data[58,59,63]: 343 cm^{-1} ν(Ag-S); 443 cm^{-1}, δ(CSS) and δ(CNC); 565 cm^{-1}, ν_{sym}(CSS) coupled to ν(S-S); 870 cm^{-1} methyl groups vi- brations; 932 cm^{-1} ν(C-S); 1149 cm^{-1}, ρ(CH_3)+ν(N–CH_3); 1386 cm^{-1} δ_{sym}(CH_3); 1454 δ_{asym}(CH_3); 1512 cm^{-1} ν(CN). In the SERS spectra, there is an apparent decrease in the band's intensity located at 565 cm^{-1}, which is the strongest band in the Raman spectrum of the thiram solution. This band is associated with disulfide linkages; thus, there is a cleavage of the S-S bond, in some extension, in the presence of the metal

colloids. Another evidence for disulfide cleavage is the absence of the band at 390 cm^{-1}, which is assigned to the S-S stretching vibration in the SERS spectra. This is in line with the absence of a similar band in the Raman spectrum of solid ziram (Figure 5), which has no disulphide bridges [55]. The SERS spectra of thiram also show a stronger band at 1512 cm^{-1}, in relation to the conventional Raman spectrum, which is indicative of the thioureide tautomer as the main metal adsorbate in the Au:Ag colloids. The SERS spectra of thiram also show the enhancement of the band at 1386 cm^{-1} arising from the short distance of the CH_3 and CN groups to the metal surface[63].

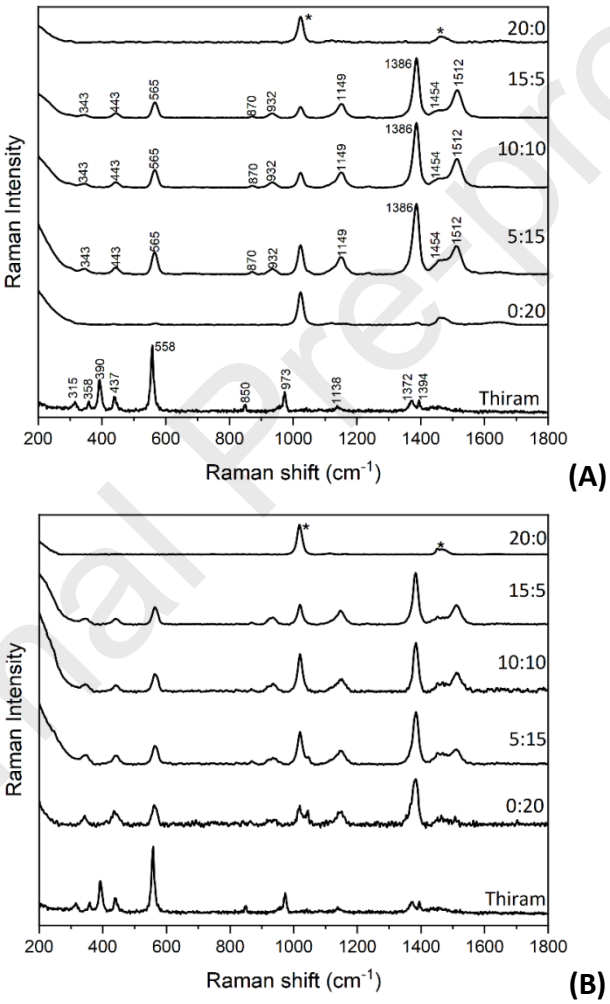

Figure 6 – Raman spectra of thiram and the corresponding SERS spectra of each colloid for the detection of thiram at $1x10^{-4}$ M using the 532 nm (A) and 633 nm (B) incident lasers. Conventional Raman spectrum of thiram powder is also shown. The band marked with an asteric arises from the residual solvent (methanol).

The lower limit of SERS detection of the dithiocarbamate pesticides was assessed using the Au:Ag colloids as substrates, as detailed in Figures 7, S9 and S10. For all the conditions tested, the SERS performance was always superior when using the excitation line at 532 nm compared to the 633 nm laser. Not only in the former case, the excitation line is more energetic, but it also better matches the spectral window of the LSPR band of the metal nanoassemblies (520-550 nm in Figure 1). It should be noted, in particular, that in these conditions, a detection limit as low as $1x10^{-7}$ M was achieved for ziram when using the nanoassemblies with 15:5:1 and 10:10:1 Au:Ag:PAMAM molar ratio. In fact, these results demonstrate a clear advantage in using the hybrid Au:Ag nanostructures as compared to the colloidal blends, for which the limit of SERS detection values were not so low (10^{-5} M for both ziram and thiram), as shown in Figures 8. According to these results, it is suggested that the PAMAM macromolecules template the formation of Au:Ag nanoassemblies, whose superior SERS activity concerning the monometallic colloids and their blends, result from the conjugation of several factors. These include a high number of open nanojunctions due to the presence of clustered metal nanoparticles, coupling of localized surface plasmons of Au:Ag nanostructures resulting in the enhancement of the localized electromagnetic field and, as previously reported by our group, the dendrimer also favours the entrapment of target molecules close to the metal surfaces promoting better SERS signal sensitivity and homogeneity (Supporting information, Figure S11) [2,44,62–65]. Also, the PAMAM dendrimer has a key role in the *in-situ* formation of these structures by providing long-term colloidal stability, which is a crucial parameter for practical applications of metal colloids in SERS detection of water pollutants. This is quite relevant by considering their integration in water remediation technologies using dendritic structures[66], which are acquiring an increasing relevance.

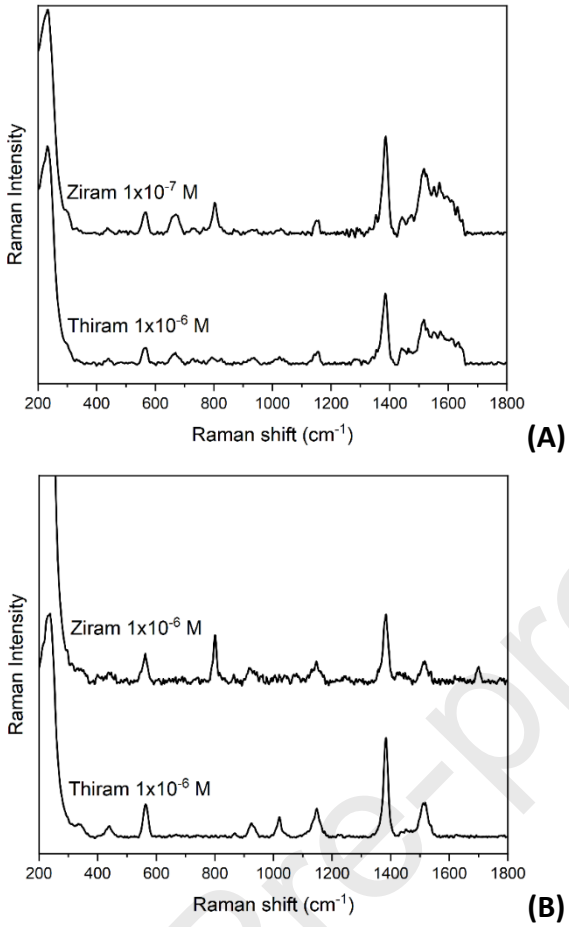

Figure 7 – SERS spectra of dithiocarbamate pesticides at distinct concentrations in the colloids, using the 15:5:1 Au:Ag:PAMAM hybrid nanostructure and the 532 nm (A) and 633 nm (B) incident lasers.

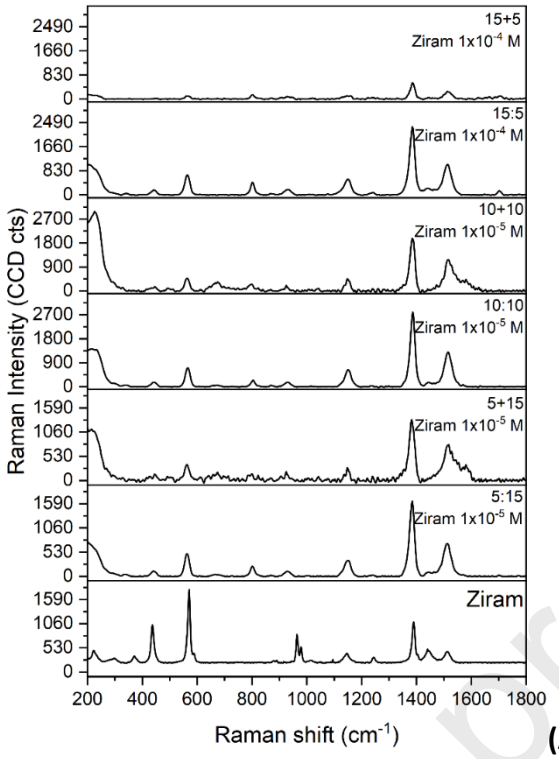

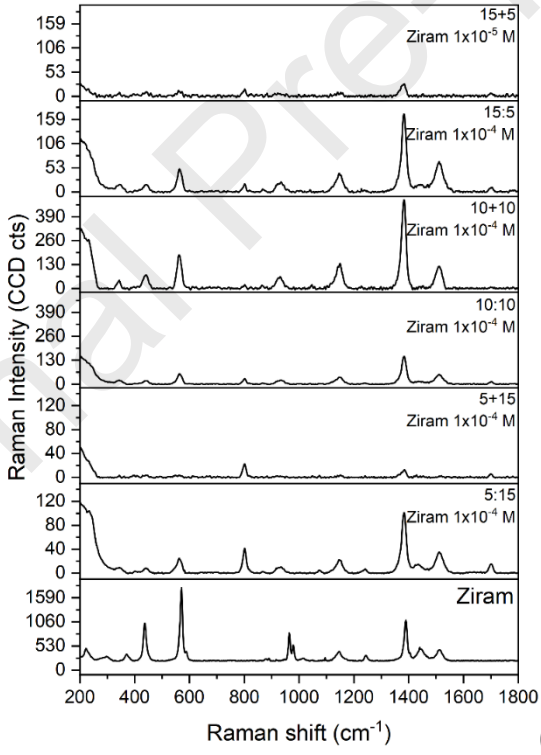

Figure 8 – SERS spectra ziram the blends of Au and Ag monometallic colloids and the corresponding binary systems taking into consideration the lowest detection limit obtained for the blends at 532 nm (A) and 633 nm (B) incident lasers. Conventional Raman spectrum of ziram are also shown.

Conclusion

Colloids of binary Au:Ag nanostructures have been prepared *in-situ* in the presence of PAMAM dendrimer, which acts both as a colloidal stabilizer and reducing agent. The resulting dendrimer coated metal colloids appear as clustered nanoparticles leading to the coupling of localized surface plasmons. This causes enhancement of the local electromagnetic field in metal nanojunctions formed, which is known to result in the enhancement of the Raman bands of molecular adsorbates at the metal surfaces. As demonstrated in this research, the *in-situ* formed Au:Ag:PAMAM nanoassemblies deliver superior performance than the corresponding monometallic systems in the SERS detection of pesticides of the dithiocarbamate family, which make these colloidal systems of interest for water quality monitoring procedures.

Acknowledgements

This work was developed within the scope of the project CICECO-Aveiro Institute of Materials, FCT Ref. UIDB/50011/2020 & UIDP/50011/2020. Tiago Fernandes thanks the Fundação para a Ciência e Tecnologia (FCT) for the PhD grant SFRH/BD/130934/2017. The costs resulting from the FCT hirings is funded by national funds (OE), through FCT, I.P. in the scope of the framework contract foreseen in the numbers 4, 5 and 6 of the article 23, of the Decree-Law 57/2016, of August 29. Ana L. Daniel-da-Silva acknowledges FCT for the research contract under the Program 'Investigador FCT' 2014.

References

[1] J.Z. Zhang, C. Noguez, Plasmonic Optical Properties And Applications Of Metal Nanostructures, Plasmonics. 3 (2008) 127–150. https://doi.org/10.1007/s11468-008-9066-y.

[2] L. Guerrini, D. Graham, Molecularly-Mediated Assemblies Of Plasmonic Nanoparticles For Surface-Enhanced Raman Spectroscopy Applications, Chem. Soc. Rev. 41 (2012) 7085–7107. https://doi.org/10.1039/C2CS35118H.

[3] J.B. Edel, A.A. Kornyshev, A.R. Kucernak, M. Urbakh, Fundamentals And Applications Of Self-Assembled Plasmonic Nanoparticles At Interfaces, Chem. Soc. Rev. 45 (2016) 1581–1596. https://doi.org/10.1039/C5CS00576K.

[4] H. Yu, Y. Peng, Y. Yang, Z.Y. Li, Plasmon-Enhanced Light–Matter Interactions And Applications, Npj Comput. Mater. 5 (2019) 45. https://doi.org/10.1038/s41524-019-0184-1.

[5] P. Karthick Kannan, P. Shankar, C. Blackman, C.H. Chung, Recent Advances In 2D Inorganic Nanomaterials For SERS Sensing, Adv. Mater. 31 (2019) 1803432. https://doi.org/10.1002/adma.201803432.

[6] H.K. Lee, Y.H. Lee, C.S.L. Koh, G.C. Phan-Quang, X. Han, C.L. Lay, H.Y.F. Sim, Y.C. Kao, Q. An, X.Y. Ling, Designing Surface-Enhanced Raman Scattering (SERS) Platforms Beyond Hotspot Engineering: Emerging Opportunities In Analyte Manipulations And Hybrid Materials, Chem. Soc. Rev. 48 (2019) 731–756. https://doi.org/10.1039/C7CS00786H.

[7] M.B. Cortie, A.M. McDonagh, Synthesis And Optical Properties Of Hybrid And Alloy Plasmonic Nanoparticles, Chem. Rev. 111 (2011) 3713–3735. https://doi.org/10.1021/cr1002529.

[8] M. Ha, J.H. Kim, M. You, Q. Li, C. Fan, J.M. Nam, Multicomponent Plasmonic Nanoparticles: From Heterostructured Nanoparticles To Colloidal Composite Nanostructures, Chem. Rev. 119 (2019) 12208–12278. https://doi.org/10.1021/acs.chemrev.9b00234.

[9] P. Dey, K.J. Thurecht, P.M. Fredericks, I. Blakey, Stepwise Like Supramolecular Polymerization of Plasmonic Nanoparticle Building Blocks through Complementary Interactions, Macromolecules. 53 (2020) 7469–7478. https://doi.org/10.1021/acs.macromol.0c01149.

[10] P. Dey, I. Blakey, K.J. Thurecht, P.M. Fredericks, Self-Assembled Hyperbranched Polymer-Gold Nanoparticle Hybrids: Understanding The Effect Of Polymer Coverage On Assembly Size And SERS Performance, Langmuir. 29 (2013) 525–533. https://doi.org/10.1021/la304034b.

[11] P. Dey, I. Blakey, K.J. Thurecht, P.M. Fredericks, Hyperbranched Polymer–Gold Nanoparticle Assemblies: Role Of Polymer Architecture In Hybrid Assembly Formation And SERS Activity, Langmuir. 30 (2014) 2249–2258. https://doi.org/10.1021/la4047462.

[12] Y. Yang, J. Zhu, J. Zhao, G.J. Weng, J.J. Li, J.W. Zhao, Growth Of Spherical Gold Satellites On The Surface Of Au@Ag@Sio_2 Core–Shell Nanostructures Used For An Ultrasensitive SERS Immunoassay Of Alpha-Fetoprotein, ACS Appl. Mater. Interfaces. 11 (2019) 3617–3626. https://doi.org/10.1021/acsami.8b21238.

[13] S. Simoncelli, E.-M. Roller, P. Urban, R. Schreiber, A.J. Turberfield, T. Liedl, T. Lohmüller, Quantitative Single-Molecule Surface-Enhanced Raman Scattering By Optothermal Tuning Of DNA Origami-Assembled Plasmonic Nanoantennas, ACS Nano. 10 (2016) 9809–9815. https://doi.org/10.1021/acsnano.6b05276.

[14] S. Tanwar, K.K. Haldar, T. Sen, DNA Origami Directed Au Nanostar Dimers for Single-Molecule Surface-Enhanced Raman Scattering, J. Am. Chem. Soc. 139 (2017) 17639–17648. https://doi.org/10.1021/jacs.7b10410.

[15] Z. Fusco, R. Bo, Y. Wang, N. Motta, H. Chen, A. Tricoli, Self-Assembly Of Au Nano-Islands With Tuneable Organized Disorder For Highly Sensitive SERS, J. Mater. Chem. C. 7 (2019) 6308–6316. https://doi.org/10.1039/C9TC01231A.

[16] S. Fateixa, H.I.S. Nogueira, T. Trindade, Surface-Enhanced Raman Scattering Spectral Imaging For The Attomolar Range Detection Of Crystal Violet In Contaminated Water, ACS Omega. 3 (2018) 4331–4341. https://doi.org/10.1021/acsomega.7b01983.

[17] D. Saviello, A. Di Gioia, P.-I. Turenne, M. Trabace, R. Giorgi, A. Mirabile, P. Baglioni, D. Iacopino, Handheld Surface-Enhanced Raman Scattering Identification Of Dye Chemical Composition In Felt-Tip Pen Drawings, J. Raman Spectrosc. 50 (2019) 222–231. https://doi.org/10.1002/jrs.5411.

[18] C. Xu, W. Lu, M. Li, Y. Cao, H. Pang, C. Gong, S. Cheng, Trifunctional Copper Mesh for Integrated Oil/Water Separation, SERS Detection, And Pollutant Degradation, Adv. Mater. Interfaces. 6 (2019) 1900836. https://doi.org/10.1002/admi.201900836.

[19] H. Lai, G. Ma, W. Shang, D. Chen, Y. Yun, X. Peng, F. Xu, Multifunctional Magnetic Sphere-MoS_2@Au Hybrid For Surface-Enhanced Raman Scattering Detection And Visible Light Photo-Fenton Degradation Of Aromatic Dyes, Chemosphere. 223 (2019) 465–473. https://doi.org/https://doi.org/10.1016/j.chemosphere.2019.02.073.

[20] J. Tang, W. Chen, H. Ju, Rapid Detection Of Pesticide Residues Using A Silver Nanoparticles Coated Glass Bead As Nonplanar Substrate For SERS Sensing, Sensors Actuators B Chem. 287 (2019) 576–583. https://doi.org/https://doi.org/10.1016/j.snb.2019.02.084.

[21] B. Hu, D.W. Sun, H. Pu, Q. Wei, Rapid Nondestructive Detection Of Mixed Pesticides Residues On Fruit Surface Using Sers Combined With Self-Modeling Mixture Analysis Method, Talanta. 217 (2020) 120998. https://doi.org/https://doi.org/10.1016/j.talanta.2020.120998.

[22] R. Li, M. Chen, H. Yang, N. Hao, Q. Liu, M. Peng, L. Wang, Y. Hu, X. Chen, Simultaneous In Situ Extraction And Self-Assembly Of Plasmonic Colloidal Gold Superparticles For SERS Detection Of Organochlorine Pesticides In Water, Anal. Chem. 93 (2021) 4657–4665. https://doi.org/10.1021/acs.analchem.1c00234.

[23] P.C. Pinheiro, S. Fateixa, H.I.S. Nogueira, T. Trindade, SERS Studies Of DNA Nucleobases Using New Silver Poly(Methyl Methacrylate) Nanocomposites As Analytical Platforms, J. Raman Spectrosc. 46 (2015) 47–53. https://doi.org/https://doi.org/10.1002/jrs.4589.

[24] H. Ma, X. Tang, Y. Liu, X.X. Han, C. He, H. Lu, B. Zhao, Surface-Enhanced Raman Scattering For Direct Protein Function Investigation: Controlled Immobilization And Orientation, Anal. Chem. 91 (2019) 8767–8771. https://doi.org/10.1021/acs.analchem.9b01956.

[25] Y. Su, D. Wu, J. Chen, G. Chen, N. Hu, H. Wang, P. Wang, H. Han, G. Li, Y. Wu, Ratiometric Surface Enhanced Raman Scattering Immunosorbent Assay Of Allergenic Proteins Via Covalent Organic Framework Composite Material Based Nanozyme Tag Triggered Raman Signal "Turn-On" And Amplification, Anal. Chem. 91 (2019) 11687–11695. https://doi.org/10.1021/acs.analchem.9b02233.

[26] Y. He, X. Yang, R. Yuan, Y. Chai, A Novel Ratiometric SERS Biosensor With One Raman Probe For Ultrasensitive Microrna Detection Based On Dna Hydrogel Amplification, J. Mater. Chem. B. 7 (2019) 2643–2647. https://doi.org/10.1039/C8TB02894J.

[27] B. Chen, G. Meng, Q. Huang, Z. Huang, Q. Xu, C. Zhu, Y. Qian, Y. Ding, Green Synthesis Of Large-Scale Highly Ordered Core@Shell Nanoporous Au@Ag Nanorod Arrays As Sensitive And Reproducible 3D SERS Substrates, ACS Appl. Mater. Interfaces. 6 (2014) 15667–15675. https://doi.org/10.1021/am505474n.

[28] A. V. Girão, P.C. Pinheiro, M. Ferro, T. Trindade, Tailoring Gold And Silver Colloidal Bimetallic Nanoalloys Towards SERS Detection Of Rhodamine 6G, RSC Adv. 7 (2017) 15944–15951. https://doi.org/10.1039/c7ra00685c.

[29] M.F. Cardinal, E. Vander Ende, R.A. Hackler, M.O. McAnally, P.C. Stair, G.C. Schatz, R.P.

Van Duyne, Expanding Applications Of Sers Through Versatile Nanomaterials Engineering, Chem. Soc. Rev. 46 (2017) 3886–3903. https://doi.org/10.1039/C7CS00207F.

[30] J. Ahn, D. Wang, Y. Ding, J. Zhang, D. Qin, Site-Selective Carving And Co-Deposition: Transformation Of Ag Nanocubes Into Concave Nanocrystals Encased By Au–Ag Alloy Frames, ACS Nano. 12 (2018) 298–307. https://doi.org/10.1021/acsnano.7b06353.

[31] G. Demirel, H. Usta, M. Yilmaz, M. Celik, H.A. Alidagi, F. Buyukserin, Surface-Enhanced Raman Spectroscopy (Sers): An Adventure From Plasmonic Metals To Organic Semiconductors As SERS Platforms, J. Mater. Chem. C. 6 (2018) 5314–5335. https://doi.org/10.1039/C8TC01168K.

[32] K. Wang, D.-W. Sun, H. Pu, Q. Wei, Shell thickness-dependent Au@Ag Nanoparticles Aggregates For High-Performance SERS Applications, Talanta. 195 (2019) 506–515. https://doi.org/https://doi.org/10.1016/j.talanta.2018.11.057.

[33] G. Barbillon, Latest Novelties On Plasmonic And Non-Plasmonic Nanomaterials For SERS Sensing, Nanomater. 10 (2020) 1200. https://doi.org/10.3390/nano10061200.

[34] C. Gao, Y. Hu, M. Wang, M. Chi, Y. Yin, Fully Alloyed Ag/Au Nanospheres: Combining The Plasmonic Property Of Ag With The Stability Of Au, J. Am. Chem. Soc. 136 (2014) 7474–7479. https://doi.org/10.1021/ja502890c.

[35] K. Liu, Y. Bai, L. Zhang, Z. Yang, Q. Fan, H. Zheng, Y. Yin, C. Gao, Porous Au–Ag Nanospheres With High-Density And Highly Accessible Hotspots For SERS Analysis, Nano Lett. 16 (2016) 3675–3681. https://doi.org/10.1021/acs.nanolett.6b00868.

[36] X.H. Pham, M. Lee, S. Shim, S. Jeong, H.-M. Kim, E. Hahm, S.H. Lee, Y.-S. Lee, D.H. Jeong, B.H. Jun, Highly Sensitive And Reliable Sers Probes Based On Nanogap Control Of A Au–Ag Alloy On Silica Nanoparticles, RSC Adv. 7 (2017) 7015–7021. https://doi.org/10.1039/C6RA26213A.

[37] K.X. Xu, X. Chen, Z. Huang, Z.N. Chen, J. Chen, J.J. Sun, Y. Fang, J.F. Li, Ligand-Free Fabrication Of Ag Nanoassemblies For Highly Sensitive And Reproducible Surface-Enhanced Raman Scattering Sensing Of Antibiotics, ACS Appl. Mater. Interfaces. 13 (2021) 1766–1772. https://doi.org/10.1021/acsami.0c16529.

[38] P. Dey, T.A. Tabish, S. Mosca, F. Palombo, P. Matousek, N. Stone, Plasmonic Nanoassemblies: Tentacles Beat Satellites For Boosting Broadband Nir Plasmon Coupling Providing A Novel Candidate For SERS And Photothermal Therapy, Small. 16 (2020) 1906780. https://doi.org/https://doi.org/10.1002/smll.201906780.

[39] X. Yan, Q. Chen, Q. Song, Z. Huo, N. Zhang, M. Ma, Continuous Mechanical Tuning Of Plasmonic Nanoassemblies For Tunable And Selective SERS Platforms, Nano Res. 14 (2021) 275–284. https://doi.org/10.1007/s12274-020-3085-1.

[40] C. Yi, Y. Yang, B. Liu, J. He, Z. Nie, Polymer-Guided Assembly Of Inorganic Nanoparticles, Chem. Soc. Rev. 49 (2020) 465–508. https://doi.org/10.1039/C9CS00725C.

[41] L.M. Bronstein, Z.B. Shifrina, Dendrimers As Encapsulating, Stabilizing, Or Directing Agents For Inorganic Nanoparticles, Chem. Rev. 111 (2011) 5301–5344. https://doi.org/10.1021/cr2000724.

[42] S. Pang, T. Yang, L. He, Review Of Surface Enhanced Raman Spectroscopic (SERS) Detection Of Synthetic Chemical Pesticides, TrAC - Trends Anal. Chem. 85 (2016) 73–82. https://doi.org/10.1016/j.trac.2016.06.017.

[43] R. Pilot, SERS Detection Of Food Contaminants By Means Of Portable Raman Instruments, J. Raman Spectrosc. 49 (2018) 954–981. https://doi.org/10.1002/jrs.5400.

[44] A. Bernat, M. Samiwala, J. Albo, X. Jiang, Q. Rao, Challenges In SERS-Based Pesticide Detection And Plausible Solutions, J. Agric. Food Chem. 67 (2019) 12341–12347. https://doi.org/10.1021/acs.jafc.9b05077.

[45] N. Kalyani, S. Goel, S. Jaiswal, On‐Site Sensing Of Pesticides Using Point‐Of‐Care Biosensors: A Review, Environ. Chem. Lett. 19 (2021) 345–354. https://doi.org/10.1007/s10311-020-01070-1.

[46] J. Choi, J.H. Kim, J.W. Oh, J.M. Nam, Surface-Enhanced Raman Scattering-Based Detection Of Hazardous Chemicals In Various Phases And Matrices With Plasmonic Nanostructures, Nanoscale. 11 (2019) 20379–20391. https://doi.org/10.1039/C9NR07439B.

[47] T. Fernandes, S. Fateixa, H.I.S. Nogueira, A.L. Daniel-da-Silva, T. Trindade, Dendrimer-Based Gold Nanostructures For SERS Detection Of Pesticides In Water, Eur. J. Inorg. Chem. n/a (2019). https://doi.org/10.1002/ejic.201901134.

[48] H. Liu, K. Sun, J. Zhao, R. Guo, M. Shen, X. Cao, G. Zhang, X. Shi, Dendrimer-Mediated Synthesis And Shape Evolution Of Gold–Silver Alloy Nanoparticles, Colloids Surfaces A Physicochem. Eng. Asp. 405 (2012) 22–29. https://doi.org/http://dx.doi.org/10.1016/j.colsurfa.2012.04.028.

[49] H. Liu, M. Shen, J. Zhao, J. Zhu, T. Xiao, X. Cao, G. Zhang, X. Shi, Facile Formation Of Folic Acid-Modified Dendrimer-Stabilized Gold–Silver Alloy Nanoparticles For Potential Cellular Computed Tomography Imaging Applications, Analyst. 138 (2013) 1979–1987. https://doi.org/10.1039/C3AN36649A.

[50] P.J.G. Goulet, D.S. Dos Santos, R.A. Alvarez-Puebla, O.N. Oliveira, R.F. Aroca, Surface-Enhanced Raman Scattering On Dendrimer/Metallic Nanoparticle Layer-By-Layer Film Substrates, Langmuir. 21 (2005) 5576–5581. https://doi.org/10.1021/la050202e.

[51] M. Frasconi, C. Tortolini, F. Botrè, F. Mazzei, Multifunctional Au Nanoparticle Dendrimer-Based Surface Plasmon Resonance Biosensor And Its Application For Improved Insulin Detection, Anal. Chem. 82 (2010) 7335–7342. https://doi.org/10.1021/ac101319k.

[52] M.P. Stemmler, Y. Fogel, K. Müllen, M. Kreiter, Bridging Of Gold Nanoparticles By Functional Polyphenylene Dendrimers, Langmuir. 25 (2009) 11917–11922. https://doi.org/10.1021/la901587e.

[53] S. Roy, C.K. Dixit, G. Manickam, S. Daniels, C. McDonagh, Dendrimer Driven Self-Assembly Of SPR Active Silver–Gold Nanohybrids, Langmuir. 29 (2013) 4430–4433. https://doi.org/10.1021/la4001285.

[54] M. Kéri, C. Peng, X. Shi, I. Bányai, NMR Characterization Of Pamam G5.Nh2 Entrapped Atomic And Molecular Assemblies, J. Phys. Chem. B. 119 (2015) 3312–3319. https://doi.org/10.1021/acs.jpcb.5b00272.

[55] J. Hu, T. Xu, Y. Cheng, NMR Insights Into Dendrimer-Based Host–Guest Systems, Chem. Rev. 112 (2012) 3856–3891. https://doi.org/10.1021/cr200333h.

[56] M. Treguer, C. de Cointet, H. Remita, J. Khatouri, M. Mostafavi, J. Amblard, J. Belloni, R. de Keyzer, Dose Rate Effects On Radiolytic Synthesis Of Gold−Silver Bimetallic Clusters In Solution, J. Phys. Chem. B. 102 (1998) 4310–4321. https://doi.org/10.1021/jp981467n.

[57] P. Vanysek, Electrochemical Series, CRC Handb. Chem. Phys. 8 (2000).

[58] S. Sánchez-Cortés, M. Vasina, O. Francioso, J. V Garćıa-Ramos, Raman And Surface-Enhanced Raman Spectroscopy Of Dithiocarbamate Fungicides, Vib. Spectrosc. 17 (1998) 133–144. https://doi.org/https://doi.org/10.1016/S0924-2031(98)00025-3.

[59] S. Sánchez-Cortés, C. Domingo, J. V García-Ramos, J.A. Aznárez, Surface-Enhanced Vibrational Study (SEIR And SERS) Of Dithiocarbamate Pesticides On Gold Films, Langmuir. 17 (2001) 1157–1162. https://doi.org/10.1021/la001269z.

[60] B. Saute, R. Premasiri, L. Ziegler, R. Narayanan, Gold Nanorods As Surface Enhanced Raman Spectroscopy Substrates For Sensitive And Selective Detection Of Ultra-Low Levels Of Dithiocarbamate Pesticides, Analyst. 137 (2012) 5082–5087. https://doi.org/10.1039/C2AN36047K.

[61] N. Hussain, H. Pu, A. Hussain, D.W. Sun, Rapid Detection Of Ziram Residues In Apple And Pear Fruits By SERS Based On Octanethiol Functionalized Bimetallic Core-Shell Nanoparticles, Spectrochim. Acta Part A Mol. Biomol. Spectrosc. 236 (2020) 118357. https://doi.org/https://doi.org/10.1016/j.saa.2020.118357.

[62] S. Fateixa, S.F. Soares, A.L. Daniel-da-Silva, H.I.S. Nogueira, T. Trindade, Silver-Gelatine Bionanocomposites For Qualitative Detection Of A Pesticide By SERS, Analyst. 140 (2015) 1693–1701. https://doi.org/10.1039/C4AN02105C.

[63] S. Fateixa, M. Raposo, H.I.S. Nogueira, T. Trindade, A General Strategy To Prepare SERS Active Filter Membranes For Extraction And Detection Of Pesticides In Water, Talanta. 182 (2018) 558–566. https://doi.org/10.1016/j.talanta.2018.02.014.

[64] R.W. Taylor, T.-C. Lee, O.A. Scherman, R. Esteban, J. Aizpurua, F.M. Huang, J.J. Baumberg, S. Mahajan, Precise Subnanometer Plasmonic Junctions For Sers Within Gold Nanoparticle Assemblies Using Cucurbit[N]Uril “Glue,” ACS Nano. 5 (2011) 3878–3887. https://doi.org/10.1021/nn200250v.

[65] A.B. Serrano-Montes, D. Jimenez de Aberasturi, J. Langer, J.J. Giner-Casares, L. Scarabelli, A. Herrero, L.M. Liz-Marzán, A General Method For Solvent Exchange Of Plasmonic Nanoparticles And Self-Assembly Into SERS-Active Monolayers, Langmuir. 31 (2015) 9205–9213. https://doi.org/10.1021/acs.langmuir.5b01838.

[66] L. Ma, Y.L. Chen, X.P. Song, D.J. Yang, H.X. Li, S.J. Ding, L. Xiong, P.L. Qin, X.B. Chen, Structure-Adjustable Gold Nanoingots With Strong Plasmon Coupling And Magnetic Resonance For Improved Photocatalytic Activity And SERS, ACS Appl. Mater. Interfaces. 12 (2020) 38554–38562. https://doi.org/10.1021/acsami.0c09684.

[67] A. Akita, M. Fujishima, H. Tada, Optical Hot Spot Generation By The Plasmonic Coupling Of Au Nanoparticles In The Nanospaces Of Mesoporous Titanium(Iv) Oxide, Langmuir. 37 (2021) 1838–1842. https://doi.org/10.1021/acs.langmuir.0c03184.

[66] M. B. Wazir, M. Daud, F. Ali, M. A. Al-Harthi, Dendrimer Assisted Dye-Removal: A Critical Review Of Adsorption And Catalytic Degradation For Wastewater Treatment, J. Mol. Liq. 315 (2020) 113775. https://doi.org/10.1016/j.molliq.2020.113775.

CRediT author statement

T. Fernandes: Investigation, Formal analysis, Methodology, Conceptualization, Writing- original draft. S. Fateixa: Investigation, Formal analysis, Writing- original draft. M. Ferro: Investigation, Writing- original draft. H. Nogueira: Validation, Resources, Writing- review & editing. A. L. Daniel-da-Silva: Conceptualization, Validation, Funding acquisition, Writing- review & editing. T. Trindade: Supervision, Conceptualization, Methodology, Resources, Funding acquisition, Writing- review & editing.

Declaration of interests

☒ The authors declare that they have no known competing financial interests or personal relationships that could have appeared to influence the work reported in this paper.

☐The authors declare the following financial interests/personal relationships which may be considered as potential competing interests:

Highlights

- Dendrimers mediate interparticle plasmonic coupling in gold:silver nanoparticles.
- Binary metal particles show better SERS performance than monometallic counterparts.
- Dendrimer metal colloidal nanoparticles for vestigial detection of pollutants.